

Nonlocal resonant inelastic x-ray scattering

Faris Gel'mukhanov,^{1,4} Ji-Cai Liu,^{2,3,*} Pavel Krasnov,⁴ Nina Ignatova,⁴ Jan-Erik Rubensson,⁵ and Victor Kimberg^{1,†}

¹*Division of Theoretical Chemistry and Biology, KTH Royal Institute of Technology, 10691 Stockholm, Sweden*

²*School of Mathematics and Physics, North China Electric Power University, 102206 Beijing, China*

³*Hebei Key Laboratory of Physics and Energy Technology, North China Electric Power University, 071000 Baoding, China*

⁴*International Research Center of Spectroscopy and Quantum Chemistry – IRC SQC, Siberian Federal University, 660041 Krasnoyarsk, Russia*

⁵*Department of Physics and Astronomy, Uppsala University, Box 516, SE-75120 Uppsala, Sweden*



(Received 15 August 2023; revised 19 October 2023; accepted 19 October 2023; published 17 November 2023)

In the description of resonant inelastic x-ray scattering (RIXS) from inversion-symmetric molecules the small core-level splitting is typically neglected. However, the spacing Δ between gerade and ungerade core levels in homonuclear diatomic molecules can be comparable with the lifetime broadening of the intermediate core-excited state Γ . We show that when $\Delta \sim \Gamma$ the scattering becomes nonlocal in the sense that x-ray absorption at one atomic site is followed by emission at the other one. This is manifested in an unusual dependence of the RIXS cross section on the sum of the momenta of incoming and outgoing x-ray photons $\mathbf{k} + \mathbf{k}'$, contrary to the normal $\mathbf{k} - \mathbf{k}'$ dependence in the conventional local RIXS theory. The nonlocality of the scattering influences strongly the scattering angle and excitation energy dependence of the intensity ratio between parity forbidden and allowed RIXS channels. Numerical simulations for N_2 show that this effect can readily be measured at present-day x-ray radiation facilities.

DOI: [10.1103/PhysRevA.108.052820](https://doi.org/10.1103/PhysRevA.108.052820)

I. INTRODUCTION

In 1801, Young [1] demonstrated the wave behavior of light by the observation of interference fringes in what became known as Young's double-slit experiment (YDSE). Similar interference fringes were later observed for electrons [2], atoms, and molecules [3]. Effects akin to YDSE were also manifested in two-center interference in photoionization [4], resonant Auger scattering [5], resonant inelastic x-ray scattering (RIXS) [6–11], and infinite-slit interference in RIXS of crystals [10,12]. One of the important fingerprints of the YDSE interference is that it opens parity-forbidden RIXS channels [6,10,13]. Another important feature of YDSE, YDSE interference fringe, was observed in resonant Auger scattering [5], hard x-ray RIXS from fixed-in-space molecules [7], and in soft x-ray RIXS from randomly oriented molecules [13].

So far, the YDSE effect in RIXS of diatomic homonuclear molecules has been studied under the assumption that the spacing between the gerade ($1\sigma_g$) and ungerade ($1\sigma_u$) core levels Δ is much smaller than the lifetime broadening Γ of the intermediate core-excited state [10]. The small value of Δ is due to the small overlap of the core orbitals localized at different atomic centers. One of the important features of

RIXS for small Δ is that the scattering cross section shows a conventional scattering dependence on the change of the photon momentum [6,10]

$$\mathbf{q} = \mathbf{k} - \mathbf{k}', \quad q \approx 2k \sin \frac{\chi}{2}, \quad (1)$$

where $\chi = \angle(\mathbf{k}, \mathbf{k}')$ is the scattering angle between the momenta of incident (\mathbf{k}) and scattered (\mathbf{k}') photons. This is because the total RIXS amplitude in this limit is a coherent sum of one-center scattering amplitudes [Fig. 1(b)] [6,10]. However, while the assumption $\Delta/2\Gamma \ll 1$ is valid in the hard x-ray region, e.g., for the Cl_2 molecule [14], it is not always justified for molecules with light elements. This is due to the fact that the increase of Δ is accompanied by the decrease of Γ on the way from heavy Cl to lighter elements, making the ratio $\Delta/2\Gamma \sim 1$ for nitrogen [15–17].

The main goal of our paper is to investigate RIXS from homonuclear diatomic molecules for arbitrary ratio $\Delta/2\Gamma$ [Fig. 1(a)]. We will show that the finite spacing Δ between the core levels of opposite parity results in an additional term in the RIXS cross section, describing a process which has so far not been considered: absorption at one atom followed by emission from the other atom of a diatomic [see Fig. 1(c)]. In contrast to the scattering theory considered so far [6,10], which implies the momentum transfer \mathbf{q} according to Eq. (1), the two-center process shows an unusual dependence on the sum of the momenta of the incoming and scattered photons

$$\mathbf{q}^+ = \mathbf{k} + \mathbf{k}', \quad q^+ \approx 2k \cos \frac{\chi}{2}, \quad (2)$$

showing qualitatively different scattering angle χ dependence, as compared to Eq. (1). We demonstrate below that, contrary to conventional scattering theory ($\Delta = 0$), the relative

*jicailiu@ncepu.edu.cn

†kimberg@kth.se

Published by the American Physical Society under the terms of the [Creative Commons Attribution 4.0 International](https://creativecommons.org/licenses/by/4.0/) license. Further distribution of this work must maintain attribution to the author(s) and the published article's title, journal citation, and DOI. Funded by [Bibsam](https://www.bibsam.org/).

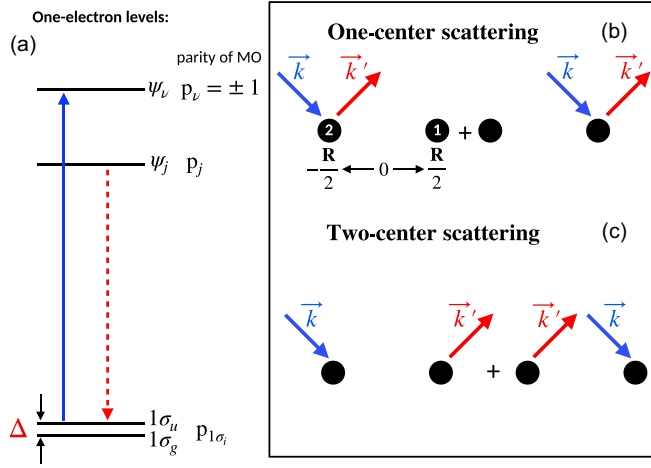


FIG. 1. (a) Scheme of RIXS transitions. (b) One-center local scattering channels, corresponding to the first term on the right-hand side of Eq. (5) (absorption and emission at the same atomic site). (c) Two-center nonlocal scattering channels, corresponding to the second term of Eq. (5) (absorption at one atomic site followed by emission from the other).

intensity of parity-forbidden RIXS band is strongly dependent on the detuning Ω of the incoming photon energy from resonance. Moreover, we will show that this unusual dependence of RIXS cross section on the sum of momenta \mathbf{q}^+ is an inherent quantum effect caused by the nonlocality of the scattering. Indeed, $\mathbf{q}^+ = \mathbf{k} + \mathbf{k}'$ describes momentum transfer to the internal degrees of freedom under nonlocal two-center scattering [Fig. 1(c)], in contrast to the local one-center scattering [Fig. 1(b)] with the momentum transfer $\mathbf{q} = \mathbf{k} - \mathbf{k}'$.

II. THEORETICAL MODEL

Homonuclear diatomic molecules have a center of symmetry at their midpoint and the electronic states of the molecule are symmetric (gerade, g) or antisymmetric (ungerade, u) with respect to inversion. We consider the RIXS process where the excitation of a core electron to an unoccupied molecular orbital (MO) $1\sigma_{u,g} \rightarrow \psi_v$ is followed by a transition from an occupied MO to the core hole $\psi_j \rightarrow 1\sigma_{u,g}$ [Fig. 1(a)]. The key feature of this process is that the scattering of an x-ray photon with frequency ω , momentum \mathbf{k} , and polarization vector \mathbf{e} proceeds via two interfering intermediate delocalized core-excited states $|c\rangle = |1\sigma_u^{-1}\psi_v^1\rangle$ and $|1\sigma_g^{-1}\psi_v^1\rangle$ of opposite parity with the energy spacing Δ

$$(\omega, \mathbf{k}) + |0\rangle \begin{cases} \rightarrow |1\sigma_u^{-1}\psi_v^1\rangle \\ \rightarrow |1\sigma_g^{-1}\psi_v^1\rangle \end{cases} \rightarrow (\omega', \mathbf{k}') + |\psi_j^{-1}\psi_v^1\rangle. \quad (3)$$

The symmetry of the core orbitals $1\sigma_i = [1s(\mathbf{r}_1) + p_i 1s(\mathbf{r}_2)]/\sqrt{2}$ and the valence orbitals $\psi_v(\mathbf{r}) = c_v\{2p_m(\mathbf{r}_1) - p_v 2p_m(\mathbf{r}_2)\} + \dots$ is characterized by the parity $p_i = 1$ and -1 for gerade and ungerade MOs, respectively, where $m = x, y$ and $m = z$ for π and σ MOs, respectively. The atomic orbitals $1s(\mathbf{r}_n)$ and $2p_m(\mathbf{r}_n)$ depend on the electron radius vector $\mathbf{r}_n = \mathbf{r} - \mathbf{R}_n$ relative to the coordinate \mathbf{R}_n of the atom

$n = 1, 2$. The small size of the core orbitals $1s(\mathbf{r}_n)$ allows us to neglect two-center integrals in the matrix elements of the absorption and emission transitions of RIXS amplitude [6,10]. In this case, simple calculations (see Appendix A) result in the following expression for partial amplitude of scattering through the gerade or ungerade core excited state ($c = g, u$):

$$\begin{aligned} F^{(c)} &= \frac{1}{Z_c} \langle 1\sigma_i | e^{-i\mathbf{k}'\cdot\mathbf{r}} (\mathbf{e}' \cdot \mathbf{r}) | \psi_j \rangle \langle \psi_v | e^{i\mathbf{k}\cdot\mathbf{r}} (\mathbf{e} \cdot \mathbf{r}) | 1\sigma_i \rangle \\ &= \frac{(\mathbf{e}' \cdot \mathbf{d}_j)(\mathbf{e} \cdot \mathbf{d}_v)}{Z_c} \left\{ e^{i(\mathbf{k}-\mathbf{k}')\cdot\mathbf{R}_1} + \mathcal{P}_f e^{i(\mathbf{k}-\mathbf{k}')\cdot\mathbf{R}_2} \right. \\ &\quad \left. - \mathcal{P}_c (\mathcal{P}_f e^{i(\mathbf{k}\cdot\mathbf{R}_1 - \mathbf{k}'\cdot\mathbf{R}_2)} + e^{i(\mathbf{k}\cdot\mathbf{R}_2 - \mathbf{k}'\cdot\mathbf{R}_1)}) \right\}, \quad (4) \end{aligned}$$

depending on the parities of the core-excited $\mathcal{P}_c = p_i p_v$ and final $\mathcal{P}_f = p_j p_v$ states. Here $Z_g = \Omega - \Delta/2 + i\Gamma$ and $Z_u = \Omega + \Delta/2 + i\Gamma$, $\Omega = \omega - (\omega_{g0} + \omega_{u0})/2$ is the frequency detuning of the incoming photon ω relative to the center between $1\sigma_g \rightarrow \psi_v$ and $1\sigma_u \rightarrow \psi_v$ absorption resonances, \mathbf{d}_v and \mathbf{d}_j are the one-center parts of the transition dipole moments of the absorption [$1s(\mathbf{r}_1) \rightarrow \psi_v$] and emission [$\psi_j \rightarrow 1s(\mathbf{r}_1)$] transitions, respectively [see Eq. (A5) of Appendix A].

The partial RIXS amplitude $F^{(c)}$ consists of two qualitatively different contributions. The first two terms of Eq. (4) describe the one-center scattering studied earlier [6,8,10,14], where the absorption is followed by the emission from the same atom [Fig. 1(b)]. The last, two-center term describes the alternative process when absorption at one atomic site is followed by emission from the other atom [Fig. 1(b)]. This process is possible since the gerade and ungerade core-hole states are delocalized. Scattering through the intermediate gerade and ungerade core-excited states ends up in the same final state (3), resulting in the sum of these two coherent paths $F_f = F^{(g)} + F^{(u)}$ in the total RIXS amplitude

$$\begin{aligned} F_f &= 2 \frac{(\mathbf{e}' \cdot \mathbf{d}_j)(\mathbf{e} \cdot \mathbf{d}_v)(\Omega + i\Gamma)}{Z_g Z_u} \\ &\quad \times \left\{ e^{i\mathbf{q}\cdot\mathbf{R}/2} + \mathcal{P}_f e^{-i\mathbf{q}\cdot\mathbf{R}/2} \right\} \\ &\quad + i \frac{\tau_c \Delta}{2} (\mathcal{P}_f e^{i\mathbf{q}^+\cdot\mathbf{R}/2} + e^{-i\mathbf{q}^+\cdot\mathbf{R}/2}) \left\{ e^{i\mathbf{q}\cdot\mathbf{R}_{CG}} \right\}. \quad (5) \end{aligned}$$

Here we take into account that $\mathbf{R}_1 = \mathbf{R}/2$ and $\mathbf{R}_2 = -\mathbf{R}/2$ in the center of the gravity frame, where $\mathbf{R} = \mathbf{R}_1 - \mathbf{R}_2$ is the interatomic radius vector. The factor $\exp(i\mathbf{q} \cdot \mathbf{R}_{CG})$ is responsible for the transfer of the momentum \mathbf{q} to the center of gravity [18] with the radius vector \mathbf{R}_{CG} . The dependence of the two-center term on the complex scattering duration $\tau_c = 1/(\Gamma - i\Omega)$ [19] reflects the dynamical origin of this contribution.

Let us single out three important differences between the conventional one-center and the additional two-center terms in Eq. (5). First, the two-center terms, being proportional to Δ , vanish when $|\tau_c|\Delta \ll 1$. Based on the assumption that $\Delta = 0$, earlier studies have thus not considered this two-center contribution [6,8,10].

Second, this additional contribution reveals a dynamical aspect of the two-center RIXS. The dependence on τ_c reflects the entanglement of the close-lying gerade and ungerade

intermediate core-excited states caused by the incoming x-ray photon, which creates a wave packet

$$\begin{aligned} \psi(t) \propto & (e^{i\mathbf{k}\cdot\mathbf{R}_1} + e^{-i\mathbf{k}\cdot\mathbf{R}_2})|u\rangle e^{-i\Delta t/2} \\ & + (e^{i\mathbf{k}\cdot\mathbf{R}_1} - e^{-i\mathbf{k}\cdot\mathbf{R}_2})|g\rangle e^{i\Delta t/2}, \end{aligned} \quad (6)$$

that describes the beating between gerade and ungerade states in the time domain, controlled by the scattering duration [10,19] $\tau = |\tau_c| = 1/\sqrt{\Omega^2 + \Gamma^2}$. The scattering duration can be varied by changing the detuning Ω in the experiment, and we will show that this allows for control of the relative contributions of the one-center and two-center RIXS channels to the scattering cross section.

Third, the nonlocal two-center channel shows a qualitatively different dependence on the photon momenta as compared to the local one-center channel. Instead of the conventional dependence on the momentum transfer $\mathbf{q} = \mathbf{k} - \mathbf{k}'$, the two-center term depends on the sum of the photon momenta $\mathbf{q}^+ = \mathbf{k} + \mathbf{k}'$. There are two important aspects of this result. The first aspect is that the YDSE interference has qualitatively different phase factors in one-center and two-center scattering

$$e^{i(\mathbf{k}-\mathbf{k}')\cdot\mathbf{R}_1} = e^{i\mathbf{q}\cdot\mathbf{R}/2}, \quad e^{i(\mathbf{k}\cdot\mathbf{R}_1 - \mathbf{k}'\cdot\mathbf{R}_2)} = e^{i\mathbf{q}^+\cdot\mathbf{R}/2}. \quad (7)$$

As one can see from Eqs. (4) and (5), the formal origin of $\mathbf{q}^+ = \mathbf{k} + \mathbf{k}'$ in the two-center scattering channels is the opposite signs of $\mathbf{R}_1 = \mathbf{R}/2$ and $\mathbf{R}_2 = -\mathbf{R}/2$. The second, physical aspect relates to the momentum transfer to the molecule in the course of scattering. The recoil momentum obtained by the molecule is shared between the momentum transfer to the center of gravity (\mathbf{q}) [18] and to the internal degrees of freedom ($\mathbf{q}/2$ and $\mathbf{q}^+/2$) followed by vibrational excitations, quantified by generalized Franck-Condon amplitudes [20] with the corresponding phase factors shown in Eq. (7). The physical picture of the two qualitatively different mechanisms of the momentum transfer to the vibrational degrees of freedom is illustrated in Fig. 2.

III. RESULTS AND DISCUSSION

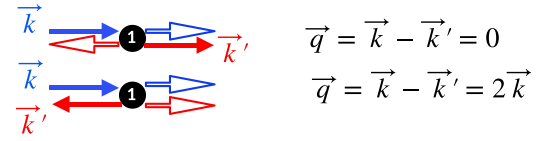
Modern x-ray coincidence techniques allow for measurements of fixed-in-space molecules [5,10,22], and scattering centers with fixed orientation are also accessible in the solid state [7]. Therefore, we first analyze fixed-in-space molecules before addressing conventional gas-phase measurements on randomly oriented species [10].

A. RIXS spectra of fixed-in-space molecules

Let us consider first the RIXS cross sections for a fixed-in-space molecule ($\sigma_f(\omega', \omega) = |F_f|^2 \Delta[\omega' - \omega + \omega_{f0}, \Gamma_f]$)

$$\begin{aligned} \sigma_f(\omega', \omega) = & \zeta_{v^*j} (\mathbf{e}' \cdot \hat{\mathbf{d}}_j)^2 (\mathbf{e} \cdot \hat{\mathbf{d}}_v)^2 \\ & \times \left\{ 1 + \mathcal{P}_f \cos(\mathbf{q} \cdot \mathbf{R}) + \frac{\Delta^2}{4(\Omega^2 + \Gamma^2)} \right. \\ & \times [1 + \mathcal{P}_f \cos(\mathbf{q}^+ \cdot \mathbf{R})] \\ & \left. - \frac{\Delta\Omega}{\Omega^2 + \Gamma^2} [\cos(\mathbf{k} \cdot \mathbf{R}) + \mathcal{P}_f \cos(\mathbf{k}' \cdot \mathbf{R})] \right\}. \end{aligned} \quad (8)$$

(a) **One-center (local) scattering** : $e^{i\mathbf{q}\cdot\mathbf{R}/2}$



(b) **Two-center (non-local) scattering** : $e^{i\mathbf{q}^+\cdot\mathbf{R}/2}$

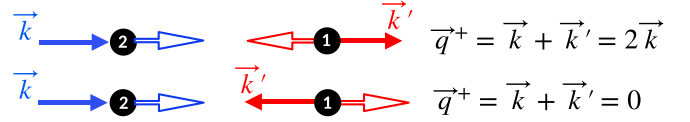


FIG. 2. Momentum exchange between x-ray photons and internal degrees of freedom (vibration). (a) In the case of one-center scattering the atom gets the momentum $\mathbf{q} = \mathbf{k} - \mathbf{k}'$ (\mathbf{k} and $-\mathbf{k}'$ are the momentum received in the course of absorption and emission, respectively). The vibrational excitation is maximal when $\mathbf{k} \uparrow \downarrow \mathbf{k}'$ ($\mathbf{q} = 2\mathbf{k}$). (b) In contrast, the total momentum transfer to the relative motion of the atoms is $\mathbf{q}^+ = \mathbf{k} + \mathbf{k}'$ in the case of the two-center scattering since the absorbing atom 2 gets the momentum \mathbf{k} , whereas the emitting atom 1 gets the momentum $-\mathbf{k}'$. The vibrational excitation is maximal when $\mathbf{k} \uparrow \uparrow \mathbf{k}'$ ($\mathbf{q}^+ = 2\mathbf{k}$). The hollow arrow shows the recoil momentum.

Here $\zeta_{v^*j} = 8d_j^2 d_v^2 (\Omega^2 + \Gamma^2) \Delta(\omega' - \omega + \omega_{f0}, \Gamma_f) / |Z_g Z_u|^2$, the Lorentzian $\Delta(\Omega, \Gamma_f)$ describes the Raman dispersion, Γ_f is the lifetime broadening of the final state, ω_{f0} is the resonant frequency of transition from the ground state to the final one, and $\hat{\mathbf{d}} = \mathbf{d}/d$. The cross section comprises three terms: The first term $[1 + \mathcal{P}_f \cos(\mathbf{q} \cdot \mathbf{R})]$ describes the local one-center scattering [6,8,10] while the second one ($\propto \Delta^2$) represents the nonlocal two-center RIXS. The interference between local and nonlocal scattering channels is given by the last term, which vanishes when $\Omega = 0$.

As a showcase for nonlocal scattering we analyze the RIXS spectra of the N_2 molecule. We focus our attention on transitions where a core electron is promoted to the π Rydberg state, $1s \rightarrow 3d\pi_g$, followed by transitions where an electron from the occupied $1\pi_u$ or $3\sigma_g$ MOs fills the core hole. Thus, we analyze the following symmetry-forbidden and symmetry-allowed RIXS channels

$$\begin{aligned} \pi^* \pi : 1s \rightarrow 3d\pi_g, \quad 1\pi_u \rightarrow 1s, \\ \text{forbidden, } \mathcal{P}_f = -1, \\ \pi^* \sigma : 1s \rightarrow 3d\pi_g, \quad 3\sigma_g \rightarrow 1s, \\ \text{allowed } \mathcal{P}_f = 1. \end{aligned} \quad (9)$$

As it is shown in Appendix [see Eq. (B1)] the cross sections for these RIXS channels read

$$\begin{aligned} \sigma_{\pi^* \pi} = & \zeta_{\pi^* \pi} [(\mathbf{e} \cdot \hat{\mathbf{d}}_{\pi_x})^2 + (\mathbf{e} \cdot \hat{\mathbf{d}}_{\pi_y})^2] \\ & \times [(\mathbf{e}' \cdot \hat{\mathbf{d}}_{\pi_x})^2 + (\mathbf{e}' \cdot \hat{\mathbf{d}}_{\pi_y})^2] \sigma_{-}, \\ \sigma_{\pi^* \sigma} = & \zeta_{\pi^* \sigma} [(\mathbf{e} \cdot \hat{\mathbf{d}}_{\pi_x})^2 + (\mathbf{e} \cdot \hat{\mathbf{d}}_{\pi_y})^2] (\mathbf{e}' \cdot \hat{\mathbf{R}})^2 \sigma_{+}. \end{aligned} \quad (10)$$

Here the subscripts in σ_{-} and σ_{+} indicate that the parities of the final states for the $\pi^* \pi$ and $\pi^* \sigma$ RIXS channels are

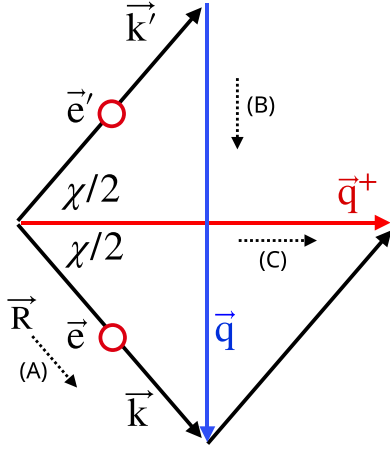


FIG. 3. Three possible orientations of the molecular axis \mathbf{R} (shown by dashed black arrow): (a) $\mathbf{R} \parallel \mathbf{k}$, (b) $\mathbf{R} \parallel \mathbf{q}$, and (c) $\mathbf{R} \parallel \mathbf{q}^+$. We consider orthogonal orientation of the polarization vectors \mathbf{e} and \mathbf{e}' (red circles) relative to the $(\mathbf{k}, \mathbf{k}')$ plane.

$\mathcal{P}_f = -1$ and $+1$, respectively. To emphasize the qualitatively different dependence of the local (σ_{\pm}^L) and nonlocal (σ_{\pm}^{NL}) scatterings on the scattering angle χ and the detuning Ω we separate the cross section into two parts

$$\begin{aligned} \sigma_{\pm} &= \sigma_{\pm}^L + \sigma_{\pm}^{\text{NL}}, \\ \sigma_{\pm}^L &= 1 \pm \cos(\mathbf{q} \cdot \mathbf{R}), \\ \sigma_{\pm}^{\text{NL}} &= \frac{\Delta^2}{4(\Omega^2 + \Gamma^2)} [1 \pm \cos(\mathbf{q}^+ \cdot \mathbf{R})] \\ &\quad - \frac{\Delta\Omega}{\Omega^2 + \Gamma^2} [\cos(\mathbf{k} \cdot \mathbf{R}) \pm \cos(\mathbf{k}' \cdot \mathbf{R})]. \end{aligned} \quad (11)$$

This equation emphasizes the difference between the local and nonlocal terms. The first depends on the conventional momentum transfer $\mathbf{q} = \mathbf{k} - \mathbf{k}'$ (1) while the nonlocal contribution shows the unusual dependence on \mathbf{k} and \mathbf{k}' and the sum of these momenta $\mathbf{q}^+ = \mathbf{k} + \mathbf{k}'$, which gives an opposite dependence on the scattering angle χ (2). This unusual dependence on χ is the fingerprint of nonlocal scattering. Note that the parity-forbidden RIXS channel ($\sigma_- \neq 0$) is opened here solely due to the YDSE interference.

The YDSE interference manifested by the \cos functions depends strongly on the mutual orientation of momenta \mathbf{q} , \mathbf{q}^+ , \mathbf{k} , and \mathbf{k}' with respect to the molecular axis \mathbf{R} . To illustrate this let consider three general cases illustrated in Fig. 3

$$\mathbf{A}: \quad \mathbf{R} \parallel \mathbf{k}, \quad (12)$$

$$\begin{aligned} \sigma_{\pm}^L &= 1 \pm \cos\left(2kR \sin^2 \frac{\chi}{2}\right), \\ \sigma_{\pm}^{\text{NL}} &= \frac{\Delta^2}{4(\Omega^2 + \Gamma^2)} \left[1 \pm \cos\left(2kR \cos^2 \frac{\chi}{2}\right) \right] \\ &\quad - \frac{\Delta\Omega}{\Omega^2 + \Gamma^2} [\cos(kR) \pm \cos(kR \cos \chi)]. \end{aligned}$$

$$\mathbf{B}: \quad \mathbf{R} \parallel \mathbf{q}, \quad (13)$$

$$\begin{aligned} \sigma_{\pm}^L &= 1 \pm \cos\left(2kR \sin \frac{\chi}{2}\right), \\ \sigma_{\pm}^{\text{NL}} &= \frac{\Delta^2}{4(\Omega^2 + \Gamma^2)} (1 \pm 1) \\ &\quad - \frac{\Delta\Omega}{\Omega^2 + \Gamma^2} \left[\cos\left(kR \sin \frac{\chi}{2}\right) \pm \cos\left(kR \sin \frac{\chi}{2}\right) \right], \\ \sigma_-^{\text{NL}} &= 0, \\ \sigma_+^{\text{NL}} &= \frac{\Delta^2}{2(\Omega^2 + \Gamma^2)} - \frac{2\Delta\Omega}{\Omega^2 + \Gamma^2} \cos\left(kR \sin \frac{\chi}{2}\right), \\ \mathbf{C}: \quad \mathbf{R} \parallel \mathbf{q}^+, \end{aligned} \quad (14)$$

$$\sigma_-^L = 0, \quad \sigma_+^L = 2,$$

$$\begin{aligned} \sigma_{\pm}^{\text{NL}} &= \frac{\Delta^2}{4(\Omega^2 + \Gamma^2)} \left[1 \pm \cos\left(2kR \cos \frac{\chi}{2}\right) \right] \\ &\quad - \frac{\Delta\Omega}{\Omega^2 + \Gamma^2} \left[\cos\left(kR \sin \frac{\chi}{2}\right) \pm \cos\left(kR \cos \frac{\chi}{2}\right) \right]. \end{aligned}$$

Cases B and C provide a nice opportunity to independently investigate local and nonlocal RIXS since $\sigma_-^{\text{NL}} = 0$ when $\mathbf{R} \parallel \mathbf{q}$ (B) while $\sigma_-^L = 0$ when $\mathbf{R} \parallel \mathbf{q}^+$ in case C.

Let us now discuss the role of the polarization of incoming \mathbf{e} and scattered \mathbf{e}' x-ray photons (10) considering the case A when $\mathbf{R} \parallel \mathbf{k}$ [Fig. 3(a)]. We fix the polarization vectors orthogonal to the molecular axis: $\mathbf{e}, \mathbf{e}' \perp \mathbf{R}$. This geometry allows to quench completely the symmetry-allowed ($\sigma_{\pi^* \sigma} = 0$) RIXS channel, as $(\mathbf{e}' \cdot \hat{\mathbf{R}}) = 0$ (Fig. 3), and thus to see only the symmetry-forbidden RIXS transition $\sigma_{\pi^* \pi} = \zeta_{\pi^* \pi} \sigma_- \neq 0$. The scattering angle dependence of σ_- together with σ_-^L and σ_-^{NL} is shown in Fig. 4 for three values of the detuning Ω .

An important fingerprint of nonlocal RIXS is that, in contrast to local RIXS (σ_-^L), the cross section of the parity-forbidden RIXS channel is not equal to zero ($\sigma_-^{\text{NL}} \neq 0$) for forward scattering ($\chi = 0$). The reason for this is the dependence of σ_-^{NL} on $\mathbf{q}^+ = \mathbf{k} + \mathbf{k}'$, \mathbf{k} , and \mathbf{k}' contrary to the local term σ_-^L which depends on the conventional momentum transfer $\mathbf{q} = \mathbf{k} - \mathbf{k}'$. Since σ_-^{NL} is the sum of the pure nonlocal scattering and interference of local and nonlocal scattering channels (12), the relative contribution of these two channels deserves a special comment. The local-nonlocal interference term is proportional to the detuning Ω , which results in the pure nonlocal contribution $\sigma_-^{\text{NL}} \propto 1 - \cos[2kR \cos^2(\chi/2)]$ when $\Omega = 0$, having opposite angular dependence as compared to the local term $\sigma_-^L \propto 1 - \cos[2kR \sin^2(\chi/2)]$. One can see nicely this opposite trend in the middle panel $\Omega = 0$ of Fig. 4. The interference between the local and nonlocal scattering channels, described by the second term ($\propto \Omega$) for σ_-^{NL} in Eq. (12), displays mixed χ dependence. Its absolute value takes the extreme at $\chi = \pi/2$ (dotted-dashed lines in Fig. 4).

B. RIXS spectra of randomly oriented molecules

The random orientation of molecules in a typical RIXS experiment modifies the YDSE pattern for a fixed-in-space

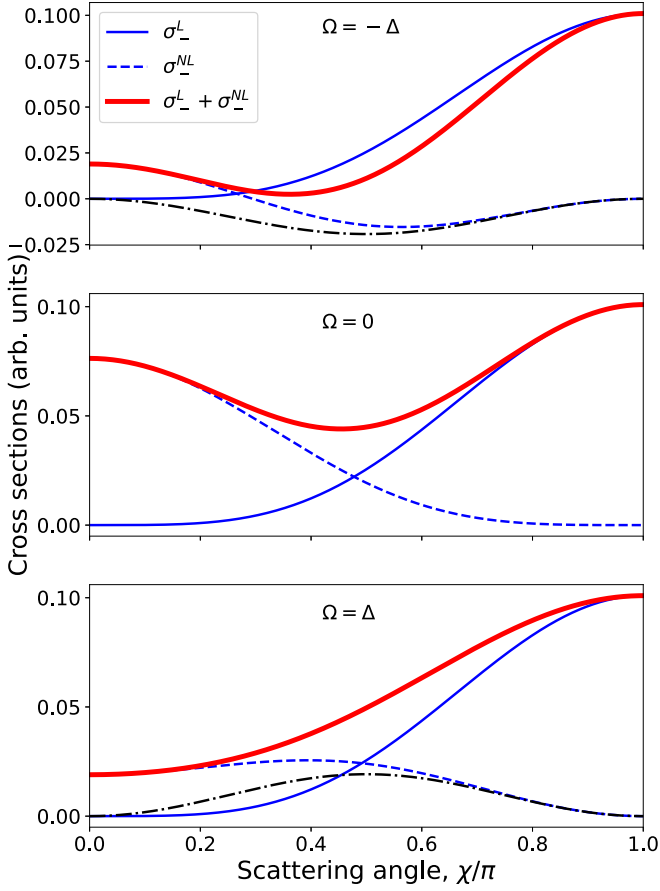


FIG. 4. RIXS for fixed-in-space molecule, case $\mathbf{R} \parallel \mathbf{k}$ [Fig. 3(a)]. The total RIXS cross section of the parity-forbidden RIXS channel $\sigma_- = \sigma_-^L + \sigma_-^{\text{NL}}$ (thick red line) is shown along with separated local σ_-^L and nonlocal σ_-^{NL} contributions computed using (12). Contrary to the local scattering the nonlocal RIXS displays almost opposite dependence on the scattering angle χ and it does not vanish for the forward scattering, $\chi = 0$. Dotted-dashed lines show the second term ($\propto \Omega$) in the expression for σ_-^{NL} (12), describing interference of the local and nonlocal scattering channels.

molecule. To take into account this effect, the cross section (8) should be averaged over molecular orientations

$$\begin{aligned} \langle \sigma_f(\omega', \omega) \rangle &= \int \sigma(\omega', \omega) \frac{d\hat{\mathbf{R}}}{4\pi} = \zeta_{v^*j} \sigma_{v^*j}, \\ \sigma_{v^*j} &= \sigma_{v^*j}^{\text{dir}} + \mathcal{P}_f \sigma_{v^*j}^{\text{int}}(\mathbf{q}) \\ &+ \frac{\Delta^2}{4(\Omega^2 + \Gamma^2)} (\sigma_{v^*j}^{\text{dir}} + \mathcal{P}_f \sigma_{v^*j}^{\text{int}}(\mathbf{q}^+)) \\ &- \frac{\Delta\Omega}{\Omega^2 + \Gamma^2} (\sigma_{v^*j}^{\text{int}}(\mathbf{k}) + \mathcal{P}_f \sigma_{v^*j}^{\text{int}}(\mathbf{k}')), \end{aligned} \quad (15)$$

where $\hat{\mathbf{R}} = \mathbf{R}/R$ is the unit vector along \mathbf{R} . We specify the final state $|f\rangle = |\psi_j^{-1} \psi_v^1\rangle$ by the indexes of the unoccupied (v^*) and occupied (j) MOs. The scattering anisotropy depends on the so-called “direct” ($\sigma_{v^*j}^{\text{dir}}$) and YDSE interference ($\sigma_{v^*j}^{\text{int}}$) terms

$$\begin{aligned} \sigma_{v^*j}^{\text{dir}} &= \overline{\langle (\mathbf{e}' \cdot \hat{\mathbf{d}}_j)^2 (\mathbf{e} \cdot \hat{\mathbf{d}}_v)^2 \rangle}, \\ \sigma_{v^*j}^{\text{int}}(\mathbf{q}) &= \overline{\langle (\mathbf{e}' \cdot \hat{\mathbf{d}}_j)^2 (\mathbf{e} \cdot \hat{\mathbf{d}}_v)^2 \cos(\mathbf{q} \cdot \mathbf{R}) \rangle}. \end{aligned} \quad (16)$$

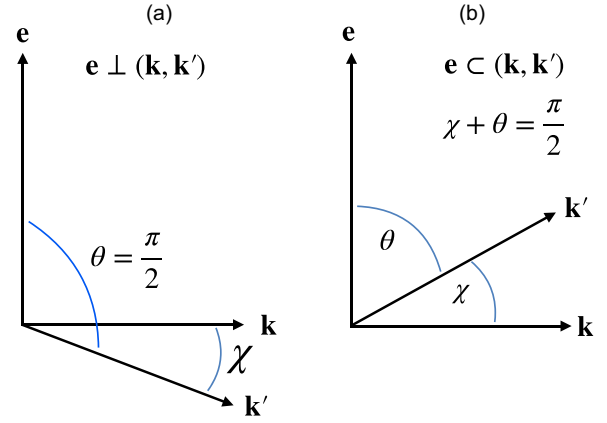


FIG. 5. (a) “Vertical” and (b) “horizontal” geometries of possible experiment.

The expressions for $\sigma_{v^*j}^{\text{int}}(\mathbf{q}^+)$, $\sigma_{v^*j}^{\text{int}}(\mathbf{k})$, and $\sigma_{v^*j}^{\text{int}}(\mathbf{k}')$ are obtained from $\sigma_{v^*j}^{\text{int}}(\mathbf{q})$ by the replacements $\mathbf{q} \rightarrow \mathbf{q}^+$, \mathbf{k}, \mathbf{k}' . The overline in Eq. (16) indicates the averaging over rotations of \mathbf{e}' around \mathbf{k}' . The reason for this averaging is that the majority of the x-ray spectrometers in soft x-ray region collect scattered photons without polarization sensitivity. The cumbersome details of the calculations of σ_f^{dir} and $\sigma_f^{\text{int}}(\mathbf{q})$ are given in Appendices B and C.

Equation (8) shows an important feature of the RIXS process: The local one-center scattering into ungerade final states ($\mathcal{P}_u = -1$) is forbidden [6,8,10,14] when $qR \approx 2kR \sin(\chi/2) \ll 1$. While this is the case in the very soft x-ray region where $2kR \ll 1$, this approximation is not fully justified at, e.g., the K edges of N_2 and O_2 , where $2kR \approx 0.44$ and $2kR \approx 0.65$, respectively. In the forward direction ($\chi = 0$) ungerade final states are forbidden in local one-center scattering also in the hard x-ray range. Nonlocal two-center scattering, on the other hand, emphasises scattering to the forbidden ungerade final states in the forward direction due to the dependence on $q^+R \approx 2kR \cos(\chi/2)$ [Eq. (8)].

The nonlocal scattering effect can be observed in the intensity ratio of the symmetry forbidden ($f = u$) and symmetry-allowed ($f = g$) RIXS bands $\sigma_{\text{forb}}/\sigma_{\text{allow}}$. To investigate the dependence on the detuning, the small splitting Δ should not be hidden by the vibrational structure of the core-excited state. This requirement is fulfilled for core excitation into the Rydberg states $3s\sigma_g, 3p\pi_u, 3d\pi_g$ of the N_2 molecule, showing no vibrational excitation [21,22]. This excitation is followed by the decay transitions from the outermost occupied MOs [23] $(2\sigma_u)^2(1\pi_u)^4(3\sigma_g)^2$.

To highlight the nonlocal scattering we compare the intensities of the symmetry-forbidden and the symmetry-allowed RIXS channels, $1s \rightarrow 3d\pi_g$; $1\pi_u \rightarrow 1s$ and $1s \rightarrow 3d\pi_g$; $3\sigma_g \rightarrow 1s$, respectively (9),

$$\frac{\sigma_{\text{forb}}}{\sigma_{\text{allow}}} = \frac{d_{1\pi_u}^2 \sigma_{\pi^*\pi}}{d_{3\sigma_g}^2 \sigma_{\pi^*\sigma}}. \quad (17)$$

According to experimental nonresonant x-ray emission spectra of the N_2 molecule [23] the ratio of transition dipole moments is equal to $d_{1\pi_u}/d_{3\sigma_g} \approx 0.79$. The derivation of the expressions for $\sigma_{\pi^*\pi} \equiv \sigma_{3d\pi_g^*1\pi_u}$ and $\sigma_{\pi^*\sigma} \equiv \sigma_{3d\pi_g^*3\sigma_g}$ can be

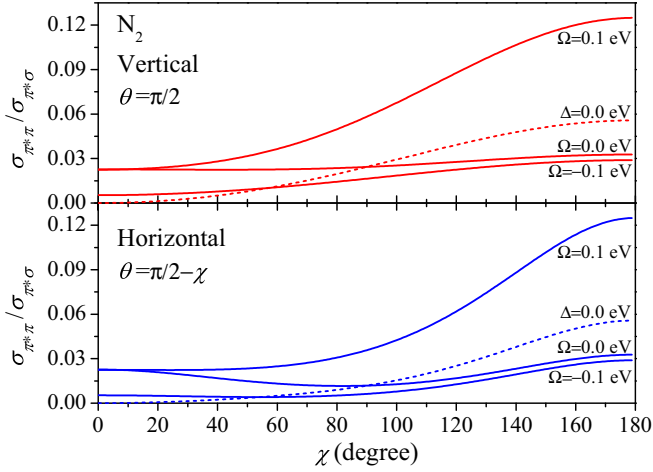


FIG. 6. Dependence of the ratio of the parity forbidden and allowed transitions $\sigma_{\pi^*\pi}/\sigma_{\pi^*\sigma}$ (17) on the scattering angle χ . The two-center contribution displays different angular dependence for different detuning Ω . In contrast, one-center local scattering ($\Delta = 0$, dashed lines) shows the angular profile independent on Ω . Following constants for the N_2 are used in the simulations: $\Delta = 0.1$ eV [15], $2\Gamma = 0.115$ eV [16,17], $\omega = 408.34$ eV [22], and $R = 2.06$ a.u.

found in Appendices B and C. Simulations are performed (see Fig. 5) for both “vertical” [$\mathbf{e} \perp (\mathbf{k}, \mathbf{k}')$; $\theta = \pi/2$] and “horizontal” [$\mathbf{e} \subset (\mathbf{k}, \mathbf{k}')$; $\theta = \pi/2 - \chi$] polarization, where $\theta = \angle(\mathbf{e}, \mathbf{k}')$ is the angle between the polarization vector \mathbf{e} of the incident radiation and the momentum \mathbf{k}' of the scattered photon.

Numerical simulations of the RIXS cross sections (Figs. 6 and 7) performed using the general Eq. (15) [see also

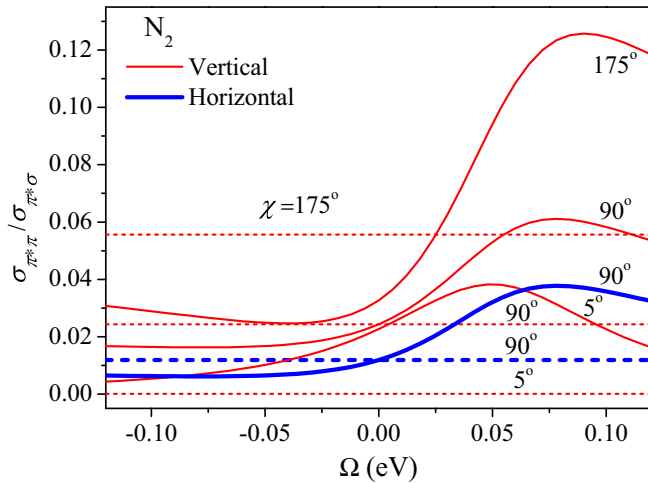


FIG. 7. Detuning Ω dependence of the ratio $\sigma_{\pi^*\pi}/\sigma_{\pi^*\sigma}$ (17) for selected scattering angles (see labels). The two-center nonlocal scattering (solid lines) provides strong dependence on the detuning Ω , in contrast to the one-center local scattering ($\Delta = 0$) shown by the dashed lines. Thin red and thick blue lines correspond to the vertical $\mathbf{e} \perp (\mathbf{k}, \mathbf{k}')$ and horizontal $\mathbf{e} \subset (\mathbf{k}, \mathbf{k}')$ polarizations, respectively. Horizontal polarization dependences for $\chi = 5^\circ$ and $\chi = 175^\circ$ are not shown here as they are almost the same as for the vertical polarization case.

Eqs. (B4), (C3) to (C5), and (C8) show strong angular and detuning dependence of the ratio (17) between the cross sections for parity-forbidden and -allowed transitions. Close to the backward scattering direction the ratio (17) reaches a sufficient value of more than 10%, which is detectable at the present-day x-ray facilities. Considered here, the N_2 system is especially suited for the experiment as the forbidden and allowed transitions are well separated in RIXS spectra [16,23]. The nonlocal and local contributions show qualitatively different angular dependence (Fig. 6). The parity selectivity is restored in the forward scattering ($\chi \rightarrow 0$) when only one-center local scattering is considered ($\Delta = 0$). In contrast (see Fig. 6), the intensity of the parity-forbidden channel is not zero when $\chi \rightarrow 0$ in the case of nonlocal two-center scattering ($\Delta \neq 0$). Moreover, the nonlocality of RIXS results in a strong detuning dependence (Fig. 7, solid lines) of the cross-section ratio (17), which is totally absent in the case of one-center local RIXS (see dashed lines).

IV. CONCLUSION

In conclusion, we demonstrated that the finite splitting of the core levels in symmetric molecules results in an additional dynamical mechanism in RIXS, where x-ray absorption at one atomic site is followed by x-ray emission from the other atom. This nonlocal scattering leads to an unusual dependence of the RIXS cross section on the sum of the momenta of incoming and outgoing x-ray photons $\mathbf{k} + \mathbf{k}'$ in contrast to the conventional scattering dependence on the momentum transfer $\mathbf{k} - \mathbf{k}'$. The simulation of the relative intensity of the symmetry forbidden RIXS channel (allowed due to Young’s double slit interference) in the N_2 molecule shows strong sensitivity to the detuning, in contrast to the conventional theory of RIXS and an unusual dependence on the scattering angle. For example, the cross section of the parity-forbidden channel is not equal to zero for the forward scattering ($\chi = 0$) contrary to the local scattering. The predictions imply that this “nonlocal” RIXS mechanism can be investigated using modern sources of intense x-ray radiation and state-of-the-art instruments. Moreover, the nonlocal character of the scattering can be studied using time-resolved measurement allowing to observe the temporal beating of the probe signal $\propto \cos \Delta t \exp(-2\Gamma t)$.

ACKNOWLEDGMENTS

The reported study was supported by STINT Mobility Grants for Internationalization, Project No. MG2021-9085. Support from the Swedish Research Council, Project No. 2019-03470, is acknowledged by V.K. and J.E.R. acknowledges support from Swedish Research Council, Project No. 2021-04017. Support from Russian Science Foundation, Project No. 21-12-00193, is acknowledged. J.-C.L. is grateful for the support by the National Natural Science Foundation of China under Grants No. 11974108 and No. 12211530044, and the Fundamental Research Funds for the Central Universities No. 2023JC005. The computations were enabled by resources provided by the National Academic Infrastructure for Supercomputing in Sweden (NAISS) at PDC and NSC partially funded by the Swedish Research Council through Grant Agreements No. 2022-06725 and No. 2018-05973.

APPENDIX A: DERIVATION OF EQ. (4) FOR FIXED-IN-SPACE MOLECULES

The partial RIXS amplitude for the homonuclear diatomic molecule is given by the Kramers-Heisenberg formula for the process shown in Eq. (3) reads

$$F^{(c)} = \frac{1}{Z_c} \langle 1\sigma_i | e^{-i\mathbf{k}' \cdot \mathbf{r}} (\mathbf{e}' \cdot \mathbf{r}) | \psi_j \rangle \langle \psi_v | e^{i\mathbf{k} \cdot \mathbf{r}} (\mathbf{e} \cdot \mathbf{r}) | 1\sigma_i \rangle, \quad (A1)$$

$$c = g, u.$$

Taking into account the wave functions of the core-shell $1\sigma_i$, unoccupied ψ_v , and occupied ψ_j molecular orbitals (MO)

$$1\sigma_i \propto 1s(\mathbf{r}_1) + p_i 1s(\mathbf{r}_2), \quad \mathbf{r}_n = \mathbf{r} - \mathbf{R}_n,$$

$$\psi_v(\mathbf{r}) = c_v \{ 2p_m(\mathbf{r}_1) - p_v 2p_m(\mathbf{r}_2) \} + \dots,$$

$$\psi_j(\mathbf{r}) = c_j \{ 2p_m(\mathbf{r}_1) - p_j 2p_m(\mathbf{r}_2) \} + \dots, \quad (A2)$$

where $p_i, p_v, p_j = \pm 1$ are the parities of corresponding MOs, $1s(\mathbf{r}_n)$ and $2p_m(\mathbf{r}_n)$ are the atomic orbitals of the n th atom with the radius vectors \mathbf{R}_n . It is worthwhile to note that, for atoms with $Z < 30$, the one-center transition matrix element can be approximated as

$$\begin{aligned} & \langle 2p_m(\mathbf{r}_n) | e^{i\mathbf{k} \cdot \mathbf{r}} | 1s(\mathbf{r}_n) \rangle \\ &= e^{i\mathbf{k} \cdot \mathbf{R}_n} \langle 2p_m(\mathbf{r}_n) | e^{i\mathbf{k} \cdot \mathbf{r}_n} | 1s(\mathbf{r}_n) \rangle \\ &\approx e^{i\mathbf{k} \cdot \mathbf{R}_n} \langle 2p_m(\mathbf{r}_n) | \mathbf{r}_n | 1s(\mathbf{r}_n) \rangle. \end{aligned} \quad (A3)$$

The small size of the $1s$ core orbital allows to neglect the two center integrals in the transition matrix elements between MOs and to write the partial scattering amplitude (A1) as

$$F^{(c)} = \frac{(\mathbf{e}' \cdot \mathbf{d}_j)(\mathbf{e} \cdot \mathbf{d}_v)}{Z_c} (e^{-i\mathbf{k}' \cdot \mathbf{R}_1} - p_i p_j e^{-i\mathbf{k}' \cdot \mathbf{R}_2}) \times (e^{i\mathbf{k} \cdot \mathbf{R}_1} - p_i p_v e^{i\mathbf{k} \cdot \mathbf{R}_2}). \quad (A4)$$

Here

$$\begin{aligned} \mathbf{d}_j &= c_j \langle 1s(\mathbf{r}) | \mathbf{r} | 2p_m(\mathbf{r}) \rangle, \\ \mathbf{d}_v &= c_v \langle 2p_m(\mathbf{r}) | \mathbf{r} | 1s(\mathbf{r}) \rangle. \end{aligned} \quad (A5)$$

This results in Eq. (4).

APPENDIX B: ORIENTATIONAL AVERAGING OF THE RIXS CROSS SECTION

Let us orient the molecular axis \mathbf{R} along z axis of molecular frame. In this case, the transition dipole moment \mathbf{d}_σ of the emission $3\sigma_g \rightarrow 1s$ transition is oriented along \mathbf{R} . The π shell consists of π_x and π_y MOs with the corresponding transition dipole moments of absorption and emission transitions \mathbf{d}_{π_x} and \mathbf{d}_{π_y} oriented orthogonal to \mathbf{R} . Thus we need to compute the cross section for the following channels (9):

$$\begin{aligned} \sigma_{\pi^* \pi} &= \langle [(\mathbf{e} \cdot \hat{\mathbf{d}}_{\pi_x})^2 + (\mathbf{e} \cdot \hat{\mathbf{d}}_{\pi_y})^2] \\ &\quad \times [(\mathbf{e}' \cdot \hat{\mathbf{d}}_{\pi_x})^2 + (\mathbf{e}' \cdot \hat{\mathbf{d}}_{\pi_y})^2] \sigma_f(\hat{\mathbf{R}}) \rangle, \\ \sigma_{\pi^* \sigma} &= \langle [(\mathbf{e} \cdot \hat{\mathbf{d}}_{\pi_x})^2 + (\mathbf{e} \cdot \hat{\mathbf{d}}_{\pi_y})^2] (\mathbf{e}' \cdot \hat{\mathbf{R}})^2 \sigma_f(\hat{\mathbf{R}}) \rangle, \end{aligned} \quad (B1)$$

where we introduce the auxiliary function

$$\begin{aligned} \sigma_f(\hat{\mathbf{R}}) &= 1 + \mathcal{P}_f \cos(\mathbf{q} \cdot \mathbf{R}) \\ &\quad + \frac{\Delta^2}{4(\Omega^2 + \Gamma^2)} [1 + \mathcal{P}_f \cos(\mathbf{q}^+ \cdot \mathbf{R})] \\ &\quad - \frac{\Delta\Omega}{\Omega^2 + \Gamma^2} [\cos(\mathbf{k} \cdot \mathbf{R}) + \mathcal{P}_f \cos(\mathbf{k}' \cdot \mathbf{R})]. \end{aligned} \quad (B2)$$

Taking into account the identity

$$(\mathbf{e} \cdot \hat{\mathbf{d}}_{\pi_x})^2 + (\mathbf{e} \cdot \hat{\mathbf{d}}_{\pi_y})^2 + (\mathbf{e} \cdot \hat{\mathbf{R}})^2 = 1, \quad (B3)$$

we obtain the following expressions for the RIXS cross-sections in terms of the unit vector $\hat{\mathbf{R}} = \mathbf{R}/R$:

$$\begin{aligned} \sigma_{\pi^* \pi} &= \sigma_{\pi^* \pi}^{\text{dir}} + \mathcal{P}_f \sigma_{\pi^* \pi}^{\text{int}}(\mathbf{q}) \\ &\quad + \frac{\Delta^2}{4(\Omega^2 + \Gamma^2)} [\sigma_{\pi^* \pi}^{\text{dir}} + \mathcal{P}_f \sigma_{\pi^* \pi}^{\text{int}}(\mathbf{q}^+)] \\ &\quad - \frac{\Delta\Omega}{\Omega^2 + \Gamma^2} [\sigma_{\pi^* \pi}^{\text{int}}(\mathbf{k}) + \mathcal{P}_f \sigma_{\pi^* \pi}^{\text{int}}(\mathbf{k}')], \\ \sigma_{\pi^* \sigma} &= \sigma_{\pi^* \sigma}^{\text{dir}} + \mathcal{P}_f \sigma_{\pi^* \sigma}^{\text{dir}}(\mathbf{q}) \\ &\quad + \frac{\Delta^2}{4(\Omega^2 + \Gamma^2)} [\sigma_{\pi^* \sigma}^{\text{dir}} + \mathcal{P}_f \sigma_{\pi^* \sigma}^{\text{int}}(\mathbf{q}^+)] \\ &\quad - \frac{\Delta\Omega}{\Omega^2 + \Gamma^2} [\sigma_{\pi^* \sigma}^{\text{int}}(\mathbf{k}) + \mathcal{P}_f \sigma_{\pi^* \sigma}^{\text{int}}(\mathbf{k}')]. \end{aligned} \quad (B4)$$

Here

$$\begin{aligned} \sigma_{\pi^* \pi}^{\text{dir}} &= \langle [1 - (\mathbf{e} \cdot \hat{\mathbf{R}})^2 - (\mathbf{e}' \cdot \hat{\mathbf{R}})^2 \\ &\quad + (\mathbf{e} \cdot \hat{\mathbf{R}})^2 (\mathbf{e}' \cdot \hat{\mathbf{R}})^2] \rangle, \\ \sigma_{\pi^* \pi}^{\text{int}}(\mathbf{q}) &= \langle [1 - (\mathbf{e} \cdot \hat{\mathbf{R}})^2 - (\mathbf{e}' \cdot \hat{\mathbf{R}})^2 \\ &\quad + (\mathbf{e} \cdot \hat{\mathbf{R}})^2 (\mathbf{e}' \cdot \hat{\mathbf{R}})^2] e^{i\mathbf{q} \cdot \mathbf{R}} \rangle, \\ \sigma_{\pi^* \sigma}^{\text{dir}} &= \langle [(\mathbf{e}' \cdot \hat{\mathbf{R}})^2 - (\mathbf{e} \cdot \hat{\mathbf{R}})^2 (\mathbf{e}' \cdot \hat{\mathbf{R}})^2] \rangle, \\ \sigma_{\pi^* \sigma}^{\text{int}}(\mathbf{q}) &= \langle [(\mathbf{e}' \cdot \hat{\mathbf{R}})^2 - (\mathbf{e} \cdot \hat{\mathbf{R}})^2 (\mathbf{e}' \cdot \hat{\mathbf{R}})^2] e^{i\mathbf{q} \cdot \mathbf{R}} \rangle. \end{aligned}$$

The equations for $\sigma_{\alpha^* \beta}^{\text{int}}(\mathbf{q}^+)$, $\sigma_{\alpha^* \beta}^{\text{int}}(\mathbf{k})$, and $\sigma_{\alpha^* \beta}^{\text{int}}(\mathbf{k}')$ are defined by the same equations as for $\sigma_{\alpha^* \beta}^{\text{int}}(\mathbf{q})$ after replacement $\mathbf{q} = \mathbf{k} - \mathbf{k}' \rightarrow \mathbf{q}^+ = \mathbf{k} + \mathbf{k}'$, \mathbf{k} , and \mathbf{k}' , respectively. Taking into account that [24]

$$\langle \hat{\mathbf{R}}_i \hat{\mathbf{R}}_j \rangle = \frac{\delta_{ij}}{3}, \quad \langle \hat{\mathbf{R}}_i \hat{\mathbf{R}}_j \hat{\mathbf{R}}_k \hat{\mathbf{R}}_l \rangle = \frac{1}{15} (\delta_{ij} \delta_{kl} + \delta_{ik} \delta_{jl} + \delta_{il} \delta_{jk}),$$

we obtain the following equation for the direct terms:

$$\begin{aligned} \sigma_{\pi^* \pi}^{\text{dir}} &= \frac{2}{15} [3 + (\mathbf{e} \cdot \mathbf{e}')^2], \\ \sigma_{\pi^* \sigma}^{\text{dir}} &= \frac{2}{15} [2 - (\mathbf{e} \cdot \mathbf{e}')^2]. \end{aligned} \quad (B5)$$

To perform the orientation averaging of the interference terms we apply the following expressions:

$$\begin{aligned} \langle e^{i\mathbf{Q} \cdot \hat{\mathbf{R}}} \rangle &= j_0(Q), \quad \mathbf{Q} = \mathbf{q}R, \\ \langle (\mathbf{e} \cdot \hat{\mathbf{R}})^2 e^{i\mathbf{Q} \cdot \hat{\mathbf{R}}} \rangle &= e_i e_j A_{ij}, \quad \langle (\mathbf{e}' \cdot \hat{\mathbf{R}})^2 e^{i\mathbf{Q} \cdot \hat{\mathbf{R}}} \rangle = e'_i e'_j A_{ij}, \\ A_{ij} &= \langle \hat{\mathbf{R}}_i \hat{\mathbf{R}}_j e^{i\mathbf{Q} \cdot \hat{\mathbf{R}}} \rangle \\ &= -\frac{\partial^2}{\partial Q_i \partial Q_j} \langle e^{i\mathbf{Q} \cdot \hat{\mathbf{R}}} \rangle = -\frac{\partial^2}{\partial Q_i \partial Q_j} j_0(Q), \end{aligned}$$

$$\begin{aligned} \langle (\mathbf{e} \cdot \hat{\mathbf{R}})^2 (\mathbf{e}' \cdot \hat{\mathbf{R}})^2 e^{i\mathbf{Q} \cdot \hat{\mathbf{R}}} \rangle &= e_i e_j e'_k e'_l B_{ijkl}, \\ B_{ijkl} &= \langle \hat{\mathbf{R}}_i \hat{\mathbf{R}}_j \hat{\mathbf{R}}_k \hat{\mathbf{R}}_l e^{i\mathbf{Q} \cdot \hat{\mathbf{R}}} \rangle = \frac{\partial^4}{\partial Q_i \partial Q_j \partial Q_k \partial Q_l} \langle e^{i\mathbf{Q} \cdot \hat{\mathbf{R}}} \rangle \\ &= \frac{\partial^4}{\partial Q_i \partial Q_j \partial Q_k \partial Q_l} j_0(Q). \end{aligned}$$

Using that $dQ/dQ_i = Q_i/Q$, the properties of the spherical Bessel functions, and that

$$\begin{aligned} (\mathbf{e} \cdot \mathbf{k}) &= (\mathbf{e}' \cdot \mathbf{k}') = 0, \\ (\mathbf{e} \cdot \mathbf{q}) &= -(\mathbf{e} \cdot \mathbf{q}^+) = -(\mathbf{e} \cdot \mathbf{k}'), \\ (\mathbf{e}' \cdot \mathbf{q}) &= (\mathbf{e}' \cdot \mathbf{q}^+) = (\mathbf{e}' \cdot \mathbf{k}), \\ (\mathbf{e} \cdot \hat{\mathbf{q}})^2 &= (\mathbf{e} \cdot \hat{\mathbf{q}}^+)^2 = \frac{k^2}{q^2} (\mathbf{e} \cdot \hat{\mathbf{k}}')^2, \end{aligned}$$

$$\begin{aligned} (\mathbf{e}' \cdot \hat{\mathbf{q}})^2 &= (\mathbf{e}' \cdot \hat{\mathbf{q}}^+)^2 = \frac{k^2}{q^2} (\mathbf{e}' \cdot \hat{\mathbf{k}})^2, \\ (\mathbf{e} \cdot \hat{\mathbf{q}})(\mathbf{e}' \cdot \hat{\mathbf{q}}) &= -\frac{k^2}{q^2} (\mathbf{e} \cdot \hat{\mathbf{k}}')(\mathbf{e}' \cdot \hat{\mathbf{k}}), \\ (\mathbf{e} \cdot \hat{\mathbf{q}})^2 (\mathbf{e}' \cdot \hat{\mathbf{q}})^2 &= \frac{k^4}{q^4} (\mathbf{e} \cdot \hat{\mathbf{k}}')^2 (\mathbf{e}' \cdot \hat{\mathbf{k}})^2, \\ (\mathbf{e} \cdot \hat{\mathbf{q}}^+)(\mathbf{e}' \cdot \hat{\mathbf{q}}^+) &= \frac{k^2}{q^2} (\mathbf{e} \cdot \hat{\mathbf{k}}')(\mathbf{e}' \cdot \hat{\mathbf{k}}), \\ (\mathbf{e} \cdot \hat{\mathbf{q}})^2 (\mathbf{e}' \cdot \hat{\mathbf{q}})^2 &= \frac{k^4}{q^4} (\mathbf{e} \cdot \hat{\mathbf{k}}')^2 (\mathbf{e}' \cdot \hat{\mathbf{k}})^2, \end{aligned}$$

we obtain the following expressions for the terms which contribute to YDSE interference terms (B5).

For $\mathbf{Q} = \mathbf{q}R$, $q = 2k \sin(\chi/2)$

$$\begin{aligned} \langle e^{i\mathbf{Q} \cdot \hat{\mathbf{R}}} \rangle &= j_0(Q), \quad \langle (\mathbf{e} \cdot \hat{\mathbf{R}})^2 e^{i\mathbf{Q} \cdot \hat{\mathbf{R}}} \rangle = \frac{j_1(Q)}{Q} - (\mathbf{e} \cdot \hat{\mathbf{k}}')^2 \frac{k^2}{q^2} j_2(Q), \quad \langle (\mathbf{e}' \cdot \hat{\mathbf{R}})^2 e^{i\mathbf{Q} \cdot \hat{\mathbf{R}}} \rangle \\ &= \frac{j_1(Q)}{Q} - (\mathbf{e}' \cdot \hat{\mathbf{k}})^2 \frac{k^2}{q^2} j_2(Q), \\ \langle (\mathbf{e} \cdot \hat{\mathbf{R}})^2 (\mathbf{e}' \cdot \hat{\mathbf{R}})^2 e^{i\mathbf{Q} \cdot \hat{\mathbf{R}}} \rangle &= [1 + 2(\mathbf{e} \cdot \mathbf{e}')^2] \frac{j_2(Q)}{Q^2} - [(\mathbf{e} \cdot \hat{\mathbf{k}}')^2 + (\mathbf{e}' \cdot \hat{\mathbf{k}})^2 - 4(\mathbf{e} \cdot \mathbf{e}')(\mathbf{e} \cdot \hat{\mathbf{k}}')(\mathbf{e}' \cdot \hat{\mathbf{k}})] \frac{k^2}{q^2} \frac{j_3(Q)}{Q} \\ &\quad + (\mathbf{e} \cdot \hat{\mathbf{k}}')^2 (\mathbf{e}' \cdot \hat{\mathbf{k}})^2 \frac{k^4}{q^4} j_4(Q), \end{aligned} \quad (\text{B6})$$

for $\mathbf{Q}^+ = \mathbf{q}^+R$, $q^+ = 2k \cos(\chi/2)$

$$\begin{aligned} \langle e^{i\mathbf{Q}^+ \cdot \hat{\mathbf{R}}} \rangle &= j_0(Q^+), \quad \langle (\mathbf{e} \cdot \hat{\mathbf{R}})^2 e^{i\mathbf{Q}^+ \cdot \hat{\mathbf{R}}} \rangle = \frac{j_1(Q^+)}{Q^+} - (\mathbf{e} \cdot \hat{\mathbf{k}}')^2 \left(\frac{k}{q^+}\right)^2 j_2(Q^+), \\ \langle (\mathbf{e}' \cdot \hat{\mathbf{R}})^2 e^{i\mathbf{Q}^+ \cdot \hat{\mathbf{R}}} \rangle &= \frac{j_1(Q^+)}{Q^+} - (\mathbf{e}' \cdot \hat{\mathbf{k}})^2 \left(\frac{k}{q^+}\right)^2 j_2(Q^+), \\ \langle (\mathbf{e} \cdot \hat{\mathbf{R}})^2 (\mathbf{e}' \cdot \hat{\mathbf{R}})^2 e^{i\mathbf{Q}^+ \cdot \hat{\mathbf{R}}} \rangle &= [1 + 2(\mathbf{e} \cdot \mathbf{e}')^2] \frac{j_2(Q^+)}{(Q^+)^2} - [(\mathbf{e} \cdot \hat{\mathbf{k}}')^2 + (\mathbf{e}' \cdot \hat{\mathbf{k}})^2 + 4(\mathbf{e} \cdot \mathbf{e}')(\mathbf{e} \cdot \hat{\mathbf{k}}')(\mathbf{e}' \cdot \hat{\mathbf{k}})] \left(\frac{k}{q^+}\right)^2 \frac{j_3(Q^+)}{Q^+} \\ &\quad + (\mathbf{e} \cdot \hat{\mathbf{k}}')^2 (\mathbf{e}' \cdot \hat{\mathbf{k}})^2 \left(\frac{k}{q^+}\right)^4 j_4(Q^+), \end{aligned} \quad (\text{B7})$$

for $\mathbf{K} = \mathbf{k}R$

$$\begin{aligned} \langle e^{i\mathbf{K} \cdot \hat{\mathbf{R}}} \rangle &= j_0(K), \quad \langle (\mathbf{e} \cdot \hat{\mathbf{R}})^2 e^{i\mathbf{K} \cdot \hat{\mathbf{R}}} \rangle = \frac{j_1(K)}{K}, \quad \langle (\mathbf{e}' \cdot \hat{\mathbf{R}})^2 e^{i\mathbf{K} \cdot \hat{\mathbf{R}}} \rangle = \frac{j_1(K)}{K} - (\mathbf{e}' \cdot \hat{\mathbf{k}})^2 j_2(K), \\ \langle (\mathbf{e} \cdot \hat{\mathbf{R}})^2 (\mathbf{e}' \cdot \hat{\mathbf{R}})^2 e^{i\mathbf{K} \cdot \hat{\mathbf{R}}} \rangle &= [1 + 2(\mathbf{e} \cdot \mathbf{e}')^2] \frac{j_2(K)}{K^2} - (\mathbf{e}' \cdot \hat{\mathbf{k}})^2 \frac{j_3(K)}{K} \end{aligned} \quad (\text{B8})$$

and for $\mathbf{K}' = \mathbf{k}'R$, $k' \approx k$

$$\begin{aligned} \langle e^{i\mathbf{K}' \cdot \hat{\mathbf{R}}} \rangle &= j_0(K), \quad \langle (\mathbf{e} \cdot \hat{\mathbf{R}})^2 e^{i\mathbf{K}' \cdot \hat{\mathbf{R}}} \rangle = \frac{j_1(K)}{K} - (\mathbf{e} \cdot \hat{\mathbf{k}}')^2 j_2(K), \quad \langle (\mathbf{e}' \cdot \hat{\mathbf{R}})^2 e^{i\mathbf{K}' \cdot \hat{\mathbf{R}}} \rangle = \frac{j_1(K)}{K}, \\ \langle (\mathbf{e} \cdot \hat{\mathbf{R}})^2 (\mathbf{e}' \cdot \hat{\mathbf{R}})^2 e^{i\mathbf{K}' \cdot \hat{\mathbf{R}}} \rangle &= [1 + 2(\mathbf{e} \cdot \mathbf{e}')^2] \frac{j_2(K)}{K^2} - (\mathbf{e} \cdot \hat{\mathbf{k}}')^2 \frac{j_3(K)}{K}. \end{aligned} \quad (\text{B9})$$

APPENDIX C: RIXS WITHOUT POLARIZATION SELECTIVITY OF THE SCATTERED PHOTONS

Majority of spectrometers in soft x-ray region collects final photons with all polarizations \mathbf{e}' . Due to this we should average the RIXS cross section over all rotations of \mathbf{e}' around \mathbf{k}' using equation [6,8,10]

$$\overline{e'_i e'_j} = \frac{1}{2}(\delta_{ij} - \hat{\mathbf{k}}'_i \hat{\mathbf{k}}'_j). \quad (\text{C1})$$

This equation results in the following expressions:

$$\begin{aligned} \overline{(\mathbf{e} \cdot \mathbf{e}')^2} &= \frac{1}{2} \sin^2 \theta, \quad (\mathbf{e} \cdot \hat{\mathbf{k}}') = \cos \theta, \\ \overline{(\mathbf{e}' \cdot \hat{\mathbf{k}})^2} &= \frac{1}{2} \sin^2 \chi, \\ \overline{(\mathbf{e} \cdot \mathbf{e}')(\mathbf{e} \cdot \hat{\mathbf{k}}')(\mathbf{e}' \cdot \hat{\mathbf{k}})} &= -\frac{1}{2} \cos^2 \theta \cos \chi, \end{aligned} \quad (\text{C2})$$

where

$$\theta = \angle(\mathbf{e}, \mathbf{k}'), \quad \chi = \angle(\mathbf{k}, \mathbf{k}').$$

Taking into account Eq. (C2) the direct terms (B5) read

$$\sigma_{\pi^*\pi}^{\text{dir}} = \frac{1}{15}(7 - \cos^2 \theta), \quad \sigma_{\pi^*\sigma}^{\text{dir}} = \frac{1}{15}(3 + \cos^2 \theta). \quad (\text{C3})$$

Taking into account Eqs. (B6), (B7), (B8), and (B9) and (C2) we get final expressions for the interference terms (B5) for the $\pi^*\pi$ RIXS channel

$$\begin{aligned} \sigma_{\pi^*\pi}^{\text{int}}(\mathbf{Q}) &= j_0(Q) - \left[2\frac{j_1(Q)}{Q} - \left(\cos^2 \theta + \frac{1}{2} \sin^2 \chi \right) \frac{k^2}{q^2} j_2(Q) \right] + \sigma_{\sigma^*\sigma}^{\text{int}}(\mathbf{Q}), \\ \sigma_{\pi^*\pi}^{\text{int}}(\mathbf{Q}^+) &= j_0(Q^+) - \left[2\frac{j_1(Q^+)}{Q^+} - \left(\cos^2 \theta + \frac{1}{2} \sin^2 \chi \right) \left(\frac{k}{q^+} \right)^2 j_2(Q^+) \right] + \sigma_{\sigma^*\sigma}^{\text{int}}(\mathbf{Q}^+), \\ \sigma_{\pi^*\pi}^{\text{int}}(\mathbf{K}) &= j_0(K) - \left[2\frac{j_1(K)}{K} - \left(\frac{1}{2} \sin^2 \chi \right) j_2(K) \right] + \sigma_{\sigma^*\sigma}^{\text{int}}(\mathbf{K}), \\ \sigma_{\pi^*\pi}^{\text{int}}(\mathbf{K}') &= j_0(K) - \left[2\frac{j_1(K)}{K} - (\cos^2 \theta) j_2(K) \right] + \sigma_{\sigma^*\sigma}^{\text{int}}(\mathbf{K}'), \end{aligned} \quad (\text{C4})$$

and for the $\pi^*\sigma$ scattering channel

$$\begin{aligned} \sigma_{\pi^*\sigma}^{\text{int}}(\mathbf{Q}) &= \frac{j_1(Q)}{Q} - \frac{1}{2} \sin^2 \chi \frac{k^2}{q^2} j_2(Q) - \sigma_{\sigma^*\sigma}^{\text{int}}(\mathbf{Q}), \\ \sigma_{\pi^*\sigma}^{\text{int}}(\mathbf{Q}^+) &= \frac{j_1(Q^+)}{Q^+} - \frac{1}{2} \sin^2 \chi \left(\frac{k}{q^+} \right)^2 j_2(Q^+) - \sigma_{\sigma^*\sigma}^{\text{int}}(\mathbf{Q}^+), \\ \sigma_{\pi^*\sigma}^{\text{int}}(\mathbf{K}) &= \frac{j_1(K)}{K} - \frac{1}{2} \sin^2 \chi j_2(K) - \sigma_{\sigma^*\sigma}^{\text{int}}(\mathbf{K}), \\ \sigma_{\pi^*\sigma}^{\text{int}}(\mathbf{K}') &= \frac{j_1(K)}{K} - \sigma_{\sigma^*\sigma}^{\text{int}}(\mathbf{K}'). \end{aligned} \quad (\text{C5})$$

Here

$$\begin{aligned} \sigma_{\sigma^*\sigma}^{\text{int}}(\mathbf{Q}) &= [1 + \sin^2 \theta] \frac{j_2(Q)}{Q^2} - \left(\cos^2 \theta + \frac{1}{2} \sin^2 \chi + 2 \cos^2 \theta \cos \chi \right) \frac{k^2}{q^2} \frac{j_3(Q)}{Q} + \frac{1}{2} \cos^2 \theta \sin^2 \chi \frac{k^4}{q^4} j_4(Q), \\ \sigma_{\sigma^*\sigma}^{\text{int}}(\mathbf{Q}^+) &= [1 + \sin^2 \theta] \frac{j_2(Q^+)}{(Q^+)^2} - \left(\cos^2 \theta + \frac{1}{2} \sin^2 \chi - 2 \cos^2 \theta \cos \chi \right) \left(\frac{k}{q^+} \right)^2 \frac{j_3(Q^+)}{Q^+} + \frac{1}{2} \cos^2 \theta \sin^2 \chi \left(\frac{k}{q^+} \right)^4 j_4(Q^+), \\ \sigma_{\sigma^*\sigma}^{\text{int}}(\mathbf{K}) &= [1 + \sin^2 \theta] \frac{j_2(K)}{K^2} - \frac{1}{2} \sin^2 \chi \frac{j_3(K)}{K}, \quad \sigma_{\sigma^*\sigma}^{\text{int}}(\mathbf{K}') = [1 + \sin^2 \theta] \frac{j_2(K)}{K^2} - \cos^2 \theta \frac{j_3(K)}{K}. \end{aligned} \quad (\text{C6})$$

We define and compute the ratio $\sigma_{\pi^*\pi}/\sigma_{\pi^*\sigma}$ (B4) for two geometries of the experiment (Fig. 5)

$$\begin{aligned} \text{vertical : } \theta &= \frac{\pi}{2}, \\ \text{horizontal : } \theta &= \frac{\pi}{2} - \chi, \end{aligned} \quad (\text{C7})$$

assuming that the $\pi^*\pi$ RIXS channel is parity forbidden while the $\pi^*\sigma$ channel is allowed:

$$\pi^*\pi : \mathcal{P}_f = -1; \quad \pi^*\sigma : \mathcal{P}_f = 1. \quad (\text{C8})$$

-
- [1] T. Young, I. The Bakerian lecture. Experiments and calculations relative to physical optics, *Philos. Trans. R. Soc.* **94**, 1 (1804).
- [2] C. J. Davisson and L. H. Germer, Reflection of electrons by a crystal of nickel, *Proc. Natl. Acad. Sci. USA* **14**, 317 (1928).
- [3] S. Eibenberger, S. Gerlich, M. Arndt, M. Mayor, and J. Tüxen, Matter-wave interference with particles selected from a molecular library with masses exceeding 10000 amu, *Phys. Chem. Chem. Phys.* **15**, 14696 (2013).
- [4] S. E. Canton, E. Plesiat, J. D. Bozek, B. S. Rude, P. Decleva, and F. Martin, Direct observation of Young's double-slit interferences in vibrationally resolved photoionization of diatomic molecules, *Proc. Natl. Acad. Sci. USA* **108**, 7302 (2011).
- [5] X.-J. Liu, Q. Miao, F. Gel'mukhanov, M. Patanen, O. Travnikova, C. Nicolas, H. Ågren, K. Ueda, and C. Miron, Einstein–Bohr recoiling double-slit gedanken experiment performed at the molecular level, *Nat. Photonics* **9**, 120 (2015).
- [6] F. Gel'mukhanov and H. Ågren, Resonant inelastic x-ray scattering with symmetry-selective excitation, *Phys. Rev. A* **49**, 4378 (1994).
- [7] A. Revelli, M. Moretti Sala, G. Monaco, P. Becker, L. Bohatý, M. Hermanns, T. C. Koethe, T. Fröhlich, P. Warzanowski, T. Lorenz, S. V. Streltsov, P. H. M. van Loosdrecht, D. I. Khomskii, J. van den Brink, and M. Grüninger, Resonant inelastic x-ray incarnation of Young's double-slit experiment, *Sci. Adv.* **5**, 2375 (2019).
- [8] F. Gel'mukhanov and H. Ågren, Resonant X-ray Raman scattering, *Phys. Rep.* **312**, 87 (1999).
- [9] L. J. P. Ament, M. Veenendaal, T. P. Devereaux, J. P. Hill, and J. Brink, Resonant inelastic x-ray scattering studies of elementary excitations, *Rev. Mod. Phys.* **83**, 705 (2011).
- [10] F. Gel'mukhanov, M. Odelius, S. P. Polyutov, A. Föhlisch, and V. Kimberg, Dynamics of resonant x-ray and Auger scattering, *Rev. Mod. Phys.* **93**, 035001 (2021).
- [11] J. Stöhr, *The Nature of X-Rays and Their Interactions with Matter*, 1st ed. (Springer, New York, 2023).
- [12] F. Kh. Gel'mukhanov, L. N. Mazalov, and N. A. Shklyaeva, Some features of x-ray fluorescence in metals near the absorption threshold, *Sov. Phys. JETP* **44**, 504 (1976).
- [13] J. Söderström, A. Ghosh, L. Kjellsson, V. Ekholm, T. Tokushima, C. Sâthe, N. Velasquez, M. Simon, O. Björneholm, L. Duda, A. Naves de Brito, M. Odelius, J. Liu, J. Wang, V. Kimberg, M. Agåker, J.-E. Rubensson, and F. Gel'mukhanov, Parity violation in resonant inelastic soft x-ray scattering at entangled core holes (unpublished).
- [14] J. D. Mills, J. A. Sheehy, T. A. Ferrett, S. H. Southworth, R. Mayer, D. W. Lindle, and P. W. Langhoff, Nondipole resonant x-ray Raman spectroscopy: Polarized inelastic scattering at the K edge of Cl₂, *Phys. Rev. Lett.* **79**, 383 (1997).
- [15] M. Ehara, H. Nakatsuji, M. Matsumoto, T. Hatamoto, X.-J. Liu, T. Lischke, and G. Prümper, T. Tanaka, C. Makochekanwa, M. Hoshino, and H. Tanaka, J. R. Harries, and Y. Tamenori, and K. Ueda, Symmetry-dependent vibrational excitation in N 1s photoionization of N₂: Experiment and theory, *J. Chem. Phys.* **124**, 124311 (2006).
- [16] J.-E. Rubensson, J. Söderström, C. Binggeli, J. Gråsjö, J. Andersson, C. Sâthe, F. Hennies, V. Bisogni, Y. Huang, P. Olalde, T. Schmitt, V. N. Strocov, A. Föhlisch, B. Kennedy, and A. Pietzsch, Rydberg-resolved resonant inelastic soft x-ray scattering: Dynamics at core ionization thresholds, *Phys. Rev. Lett.* **114**, 133001 (2015).
- [17] L. Kjellsson, V. Ekholm, M. Agåker, C. Sâthe, A. Pietzsch, H. O. Karlsson, N. Jaouen, A. Nicolaou, M. Guarise, C. Hague, J. Lüning, S. G. Chiuzbăian, and J.-E. Rubensson, Resonant inelastic x-ray scattering at the N₂ π^* resonance: Lifetime-vibrational interference, radiative electron rearrangement, and wave-function imaging, *Phys. Rev. A* **103**, 022812 (2021).
- [18] V. C. Felicíssimo, F. F. Guimares, and F. Gel'mukhanov, Enhancement of the recoil effect in x-ray photoelectron spectra of molecules driven by a strong ir field, *Phys. Rev. A* **72**, 023414 (2005).
- [19] F. Gel'mukhanov, P. Sałek, T. Privalov, and H. Ågren, Duration of x-ray Raman scattering, *Phys. Rev. A* **59**, 380 (1999).
- [20] P. Sałek, F. Gel'mukhanov, H. Ågren, O. Björneholm, and S. Svensson, Generalized Franck-Condon principle for resonant photoemission, *Phys. Rev. A* **60**, 2786 (1999).
- [21] M. Neeb, J.-E. Rubensson, M. Biermann, and W. Eberhardt, Coherent excitation of vibrational wave functions observed in core hole decay spectra of O₂, N₂ and CO, *J. Electron Spectrosc. Relat. Phenom.* **67**, 261 (1994).
- [22] J.-I. Adachi, N. Kosugi, and A. Yagishita, Symmetry-resolved soft x-ray absorption spectroscopy: Its application to simple molecules, *J. Phys. B: At. Mol. Opt. Phys.* **38**, R127 (2005).
- [23] P. Glans, P. Skytt, K. Gunnelin, J.-H. Guo, and J. Nordgren, Selectively excited X-ray emission spectra of N₂, *J. Electron Spectrosc. Relat. Phenom.* **82**, 193 (1996).
- [24] D. A. Varshalovich, A. N. Moskalev, and A. N. Khersonskii, *Quantum Theory of Angular Momentum* (World Scientific, Singapore, 1988).